Parameter Configuration Scheme for Optimal Energy Efficiency in LoRa-Based Wireless Underground Sensor Networks

Huaijin Zhang, *Graduate Student Member, IEEE*, Guanghua Liu, *Member, IEEE*, and Tao Jiang, *Fellow, IEEE*

***Abstract*—Long Range (LoRa)-based wireless underground sensor networks (WUSNs) have attracted much attention due to their long-range communication capability and easiness of deployment. Since it is difficult to replace batteries in buried end nodes, energy efficiency (EE) needs to be improved to extend the lifespan. As link quality is closely related to LoRa physical layer (PHY) parameters and soil characteristics, it is necessary to carefully configure parameters to maintain reliable connectivity and high EE in the dynamic underground environment. To this end, we propose EnergySaver, which utilizes soil moisture to estimate the underground path loss, derives signal-to-noise ratio (SNR) to characterize the packet delivery rate (PDR), and finally calculates EE. The combination that maximizes EE is the best configuration for current channel state. In addition, for the case of densely deployed buried LoRa nodes, we propose a low-complexity collision decoding scheme in EnergySaver that utilizes packet time offsets to decompose concurrent transmissions. The simulation results confirm that EnergySaver improves EE by at least two times without sacrificing high link quality, and effectively reduces packet loss during concurrent data transmission with excellent scalability.**

***Index Terms*—Wireless underground sensor networks, Long Range (LoRa), energy efficiency, adaptive parameter configuration, collision decoding.**

I. Introduction

In order to effectively utilize natural resources in underground environment, researchers have developed a strong interest in wireless underground sensor networks (WUSNs) [1], [2]. Due to the resource constraints and dramatic signal degradation in underground environment, the communications of WUSNs face serious challenges. Fortunately, LoRa (Long Range) technology, with its obvious advantages of high reception sensitivity, ultra-low power consumption, and low cost, is ideally suited as a new communication solution for WUSNs. Many preliminary applications of LoRa-based WUSNs have emerged in recent years [3], [4], [5], [6], which can effectively improve the signal reception quality. However, due to high attenuation in harsh underground soils, LoRa devices require more energy to communicate with aboveground gateways for reliable data transmission. If the design is based on the worst-case scenario, although reliable communication is guaranteed, more serious energy consumption problems arise because the sensor nodes are buried underground, making it difficult to replace the batteries [5]. Therefore, the problem of balancing link reliability and energy efficiency (EE) in a dynamic underground environment is critical for LoRa-based WUSNs. Furthermore, for application scenarios such as greenhouses, where LoRa nodes are deployed very densely, it is likely that multiple nodes communicate with the gateway concurrently, resulting in packet loss and retransmission. Therefore, how to resolve collisions is also a challenge to improve EE.

There has been much research on adaptive adjustment of LoRa physical layer (PHY) parameters to save energy, the most famous of which is the adaptive data rate (ADR) mechanism provided by LoRaWAN [7]. However, it typically requires several days to gather link information and make configuration changes, making it inflexible for the rapidly changing underground environment. To cope with variable channel conditions, [8] proposes an improved version of the original ADR mechanism, called ND-ADR. However, both ADR and ND-ADR tend to use longer transmission duration and higher transmit power (TP) to ensure reliability, making it difficult to achieve optimal EE. The ALPPS mechanism proposed in [5] can effectively avoid these problems and reduce the total power consumption by more than 60%. However, it depends strongly on the value of the interference coefficient K, which is empirically determined and varies in different underground environments. Furthermore, a multi-agent reinforcement learning (MARL)-based algorithm is proposed in [4] for selecting parameters in large-scale LoRa-based WUSNs. Although this approach is inspiring, using RL is not cost-effective in terms of time and energy resources. In addition, although the scheme takes collisions into account, it does not decode the colliding packets, which still leads to retransmission of packets, thus reducing EE.

In this work, a parameter selection mechanism for optimal EE is proposed in the resource-constrained LoRa-based WUSNs. Specifically, given the volumetric water content (VWC) of soil measured by soil moisture sensor, the signal-to-noise ratio (SNR) can be estimated and further used to calculate the link reliability indicator. The EE is determined together by packet delivery rate (PDR), data rate (DR), and TP. By using the underground channel model and LoRa transmission characteristics, the closed-form expression for EE is also derived. Afterwards, the optimal parameter configuration for the current channel state can be obtained by selecting the combination that maximizes EE. In addition, for the collision problem that is highly prone to occur when buried LoRa nodes are densely deployed, we propose a low-complexity collision decoding scheme that utilizes packet time offsets to decompose concurrent transmissions in a single collision. Our simulation results show that EnergySaver has significant advantages over existing selection algorithms, which can improve EE more than two times while maintaining the reliable connection. In addition, EnergySaver can effectively reduce packet loss and retransmission during large concurrent data transmission, and has excellent scalability.

II. Channel Model of WUSNs

In our considered scenario, the gateway tracks link quality based on packets sent by node, selects the best parameter settings in real time, and then gives feedback to node. Therefore, we only consider the case of underground-to-aboveground (UG2AG), i.e., the uplink. Based on the path loss characterization of the UG channel, the link budget of the channel can be modeled as follows

$$P_r = \mathrm{TP} + G_t + G_r - P_L, \tag{1}$$

Received 27 December 2023; revised 13 June 2024 and 4 November 2024; accepted 6 February 2025. Date of publication 17 February 2025; date of current version 20 June 2025. This work was supported in part by the National Natural Science Foundation of China under Grant 62371200, in part by the National Key Research and Development Program of China under Grant 2024YFB2908802 and in part by Young Elite Scientists Sponsorship Program by CAST under Grant 2023QNRC001. The review of this article was coordinated by Dr. Shiva Raj Pokhrel. *(Corresponding author: Guanghua Liu.)*

The authors are with the Research Center of 6G Mobile Communications, School of Cyber Science and Engineering, Huazhong University of Science and Technology, Wuhan 430074, China, and also with the School of Electronic Information and Communications, Huazhong University of Science and Technology, Wuhan 430074, China (e-mail: huaijinzhang@hust.edu.cn; guanghualiu@hust.edu.cn; tao.jiang@ieee.org).

Digital Object Identifier 10.1109/TVT.2025.3540462

where P_r is the received power, TP is the transmit signal power, G_t is the gain of transmitting antenna and G_r is the gain of receiving antenna. P_L is the path loss of UG-AG channel. It consist of three parts: the path loss L_{UG} in soil, the path loss L_{AG} in air and the refraction loss $L_{\text{UG,AG}}$ at the soil-air interface [9].

$$P_L = L_{\text{UG}}(d_{\text{UG}}) + L_{\text{AG}}(d_{\text{AG}}) + L^R_{\text{UG,AG}}, \tag{2}$$

$$L_{UG}(d_{\text{UG}}) = 6.4 + 20\log d_{\text{UG}} + 20\log\beta + 8.69\alpha d_{\text{UG}}, \tag{3}$$

$$L_{AG}(d_{\text{AG}}) = -147.6 + 20\log d_{\text{AG}} + 20\log f_c. \tag{4}$$

$$L_{UG,AG} \simeq 10\log\frac{\left(\sqrt{\epsilon'}+1\right)^2}{4\sqrt{\epsilon'}}. \tag{5}$$

The values of the attenuation constant $\alpha = 2\pi f_c\sqrt{\frac{\mu\epsilon'}{2}[\sqrt{1+(\frac{\epsilon''}{\epsilon'})^2}-1]}$ and the phase shifting constant $\beta = 2\pi f_c\sqrt{\frac{\mu\epsilon'}{2}[\sqrt{1+(\frac{\epsilon''}{\epsilon'})^2}+1]}$ depend on the dielectric properties of soil. In the expressions, f_c is the central frequency, μ is the magnetic permeability, ϵ' and ϵ'' are the real and imaginary parts of the relative dielectric constant of soil-water mixture, which mainly depend on the VWC of soil, the mass fraction of sand, denoted as S, and the mass fraction of clay, denoted as C. In UG2AG communication, d_{AG} and d_{UG} represent the path length of AG and UG respectively, h_u is the burial depth, h_a is the height of gateway, and d is the horizontal distance between node and gateway. Since $d_{\text{AG}} >> h_a$, the incident angle θ_I is approximately equal to the critical angle $\theta_C \simeq arcsin\frac{1}{\sqrt{\epsilon'}}$, and the refracted angle θ_R is approximately equal to 90°. In this case, $d_{\text{AG}} \simeq d$ and $d_{\text{UG}} \simeq \frac{h_u}{cos(\theta_C)}$ hold.

With the given soil characteristic parameters and node location information, signal attenuation value can be estimated based on the above channel model.

III. System Design

In this section, we first briefly introduce the system structure and the factors influencing EE. After that, the calculation of PDR is highlighted and the closed-form expression of EE is given accordingly. Then, a scheme for selecting the optimal parameter configuration is presented. Finally, a collision decoding scheme is proposed to avoid retransmission.

A. System Overview

There are four physical parameters that affect LoRa performance: TP, spread factor (SF), bandwidth (BW), and code rate (CR) [6]. Therefore, we propose the EnergySaver system to achieve reliable transmission with maximum EE by selecting the optimal parameter configuration for the current channel state. Specifically, for each possible combination, the gateway takes the soil moisture, node location, and current TP into the underground channel model to compute the SNR. Then, the obtained SNR and LoRa PHY parameters are used to compute the EE and the configuration that optimizes EE will be selected. In particular, we require that the selected parameter configuration needs to satisfy a PDR greater than 90% to ensure high quality of the link. Otherwise, the transmission is considered to be failed with EE being 0. Finally, the gateway sends the selected configuration back to the buried node. If multiple nodes send packets concurrently and collisions occur at the gateway, the collision decoding algorithm is performed using the unaligned window, thus avoiding packet discarding and retransmission. The specific steps are detailed in Section III-D. To summarize, the EnergySaver system architecture is shown in Fig. 1.

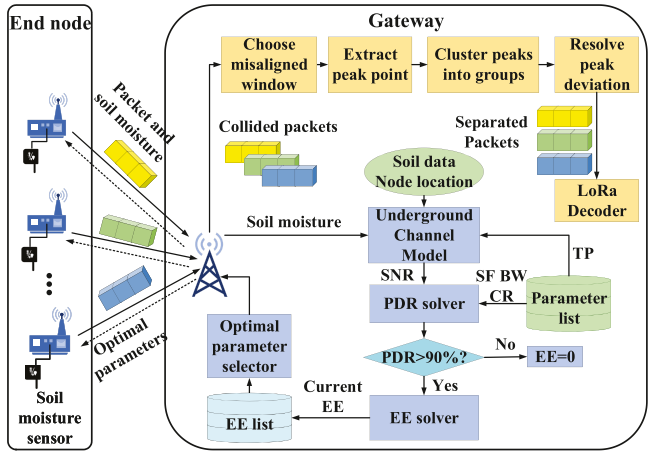

Fig. 1. System architecture of EnergySaver.

TABLE I
Relevant Parameters for EE Calculation

Parameter	Notation	Parameter	Notation
Burial depth	h_u	Central frequency	f_c
Horizontal distance	d	Length of preamble	n
Height of gateway	h_a	Length of header	L_h
Mass fraction of sand	S	Length of payload	L_p
Mass fraction of clay	C	Unencoded LoRa symbol error rate	P_s
Gain of transmitter	G_t	SNR	γ
Gain of receiver	G_r	Underground noise power	P_n

EE (unit: bits/Joule) is the number of bits successfully transmitted per unit of energy in the entire network, determined by three parameters jointly [10],

$$\text{EE} = \frac{\text{DR}\cdot\text{PDR}}{\text{TP}}. \tag{6}$$

Therein, PDR represents the reliability of transmission and its value is the ratio of correctly decoded packets to the total number of packets sent. The DR of LoRa, determined by SF, BW, and CR together, is denoted as

$$\text{DR} = \text{SF} * \frac{4\text{BW}}{(4+\text{CR})2^{\text{SF}}}. \tag{7}$$

The EE of system is proportional to DR and PDR and inversely proportional to TP. Since the acquisition of DR and TP is relatively straightforward, the most important aspect is the calculation of PDR. Since we use a large number of symbols in our derivation, we provide a notation Table I here for clarity and ease of reference.

B. The Calculation of PDR

The LoRa packet contains three components: preamble, header, and payload. The preamble is utilized for synchronization purposes. It consists of $n+2$ upchirps (we set n to 8), and then ends with a start frame delimiter (SFD) of 2.25 downchirps. The header contains structure information and exists in explicit mode. The payload is where the message is encoded. The successful reception of a packet requires all three to be demodulated simultaneously.

1) Detection Probability of Preamble: LoRa performs correlation operation on preamble to determine whether the signal has arrived. The correlation operation has the same gain and detection probability as LoRa demodulation. Therefore, the unencoded LoRa symbol error

rate P_s can be denoted as

$$P_s \approx Q\left(\sqrt{\gamma \cdot 2^{\mathrm{SF}+1}} - \sqrt{1.386 \cdot \mathrm{SF} + 1.154}\right), \tag{8}$$

with $Q(x) = \frac{1}{\sqrt{2\pi}} \cdot \int_x^{\infty} \exp[-\frac{u^2}{2}]du$ being the Q-function, that is, the tail function of standard normal distribution. The above equation shows that PDR is highly correlated with SNR. Because SNR is determined by environment and TP, we consider using the underground channel model described in Section II to obtain the desired SNR in the form of dB

$$\gamma_{dB} = P_r - P_n = \mathrm{TP} + G_t + G_r - P_L - P_n, \tag{9}$$

where P_n is characterized empirically to be around -110 dBm [3]. Once the soil characteristic parameters and node deployment locations are determined, SNR is only related to the value of TP, and (8) can be rewritten as

$$P_s(\mathrm{TP}, \mathrm{SF}) \approx Q\left(\sqrt{10^{\frac{(\mathrm{TP}+G_t+G_r-P_L-P_n)}{10}} \cdot 2^{\mathrm{SF}+1}} - \sqrt{1.386 \cdot \mathrm{SF} + 1.154}\right), \tag{10}$$

Considering the preamble as a LoRa symbol modulated with spreading factor $\mathrm{SF} + \log_2(n + 4.25)$, the detection probability can be modeled as

$$P_{\text{preamble}}(\mathrm{TP}, \mathrm{SF}) = 1 - P_s(\mathrm{TP}, \mathrm{SF} + \log_2(n + 4.25)) \tag{11}$$

2) Detection Probability of Header: LoRa utilizes Hamming codes for forward error correction. The header has a fixed coding rate of $4/8$, which means that 4 redundant bits are added for every 4 data bits. These 4 redundant bits can correct at most 1 b error. Therefore, the decoding probability of header is given as

$$P_{\text{header}}(\mathrm{TP}, \mathrm{SF}) = \left((1 - P_s)^4 + 3(1 - P_s)^7 P_s\right)^{\left\lceil \frac{L_h}{4\mathrm{SF}} \right\rceil}. \tag{12}$$

3) Detection Probability of Payload: For the payload, $\mathrm{CR} = 4/5$ and $\mathrm{CR} = 4/6$ can only detect bit errors without correcting them, while $\mathrm{CR} = 4/7$ and $\mathrm{CR} = 4/8$ can correct 1 b error for every 4 bits. Therefore, we can calculate the decoding probability of payload corresponding to different CR as follows

$$P_{\text{payload}}(\mathrm{TP}, \mathrm{SF}) = \begin{cases} (1 - P_s)^{\left\lceil \frac{L_p}{\mathrm{SF}} \right\rceil}, \mathrm{CR} = 4/5, 4/6 \\ \left((1 - P_s)^4 + 3(1 - P_s)^{3+\mathrm{CR}} P_s\right)^{\left\lceil \frac{L_p}{4\mathrm{SF}} \right\rceil}, \mathrm{CR} = 4/7, 4/8. \end{cases} \tag{13}$$

Then PDR can be calculated as the product of the above three probabilities as follows

$$\mathrm{PDR}(\mathrm{TP}, \mathrm{SF}) = P_{\text{preamble}} \times P_{\text{header}} \times P_{\text{payload}}. \tag{14}$$

Combining the above analysis, the closed-form expressions for EE affected by each parameter can be derived as (15), shown at the bottom of this page. From the closed-form expression, it can be concluded that once the soil characteristics, node location and LoRa packet structure are determined, the value of EE is determined by SF, TP, BW, and CR together.

Algorithm 1: Parameter Selection of EnergySaver.

Input: $d, h_u, h_a, G_t, G_r, f_c, S, C, P_n$, CR, n, L_h, L_p;
Output: TP, SF, BW, PDR, EE

```
Calculate the path loss P_L using Eq. (2)-(4)
for TP in TP_list do
    Obtain the SNR γ = 10^((P_r − P_n)/10) = 10^((TP+G_t+G_r−P_L−P_n)/10)
    for SF in SF_list, BW in BW_list do
        DR = SF * 4BW / ((4+CR)2^SF)
        Substitute γ, SF, n, CR, L_h, L_p into Eq. (11)-(14) to
          obtain PDR
        if PDR > 90% then
            EE = DR·PDR / TP
            if EE is optimal then
                Return TP, SF, BW
            end
        end
        else
            EE=0, Transmission Failed
        end
    end
end
```

C. Optimal Parameter Selection Mechanism

Our goal is to maximize EE of the system as much as possible while maintaining transmission reliability. In particular, we require that the selected parameter configuration needs to satisfy a PDR greater than 90% to ensure high quality of the link. Otherwise, the transmission is considered to be failed with EE being 0. Briefly, the problem of finding the parameter combination that enables the maximum EE can be formulated as an optimization problem, as shown in (16).

$$\max_{\mathrm{SF},\mathrm{TP},\mathrm{BW},\mathrm{CR}} \mathrm{EE}, \quad \text{s.t. } \mathrm{PDR} > 90\% \quad \mathrm{SF} \in \mathrm{SF}_{\text{list}}, \mathrm{BW} \in \mathrm{BW}_{\text{list}}, \mathrm{TP} \in \mathrm{TP}_{\text{list}}, \mathrm{CR} \in \mathrm{CR}_{\text{list}} \tag{16}$$

where $\mathrm{SF}_{\text{list}}, \mathrm{BW}_{\text{list}}, \mathrm{TP}_{\text{list}}$, and $\mathrm{CR}_{\text{list}}$ represent the ranges of values of SF, BW, TP, and CR, respectively. In order to obtain the best configuration, EE corresponding to all possible combinations of parameters needs to be solved, and the solution that maximizes EE is finally chosen. The pseudo-code for EnergySaver is provided in Algorithm 1. In practice, this process has to be executed once whenever the link undergoes a dynamic change.

D. Decoding of Collision Packets

When multiple LoRa devices use the same parameters (e.g., channel and SF) to communicate with the gateway, they are prone to conflicts, severely limiting network throughput and scalability. We propose a collision decoding algorithm in EnergySaver to decompose concurrent transmissions. For the sake of illustration, we assume that there are R collision packets and the total number of reception windows is Q. The core of the algorithm utilizes packet time offsets and consists of the following components.

$$\mathrm{EE} = \begin{cases} \frac{\mathrm{SF}\times 4\mathrm{BW}\times[1-P_s(\mathrm{TP},\mathrm{SF}+\log_2(n+4.25))]\times[\left((1-P_s)^4+3(1-P_s)^7P_s\right)^{\left\lceil \frac{L_h}{4\mathrm{SF}} \right\rceil}\times(1-P_s)^{\left\lceil \frac{L_p}{\mathrm{SF}} \right\rceil}]}{\mathrm{TP}\times(4+\mathrm{CR})2^{\mathrm{SF}}}, \mathrm{CR} = \frac{4}{5}, \frac{4}{6} \\ \frac{\mathrm{SF}\times 4\mathrm{BW}\times[1-P_s(\mathrm{TP},\mathrm{SF}+\log_2(n+4.25))]\times[\left((1-P_s)^4+3(1-P_s)^7P_s\right)^{\left\lceil \frac{L_h}{4\mathrm{SF}} \right\rceil}\times\left((1-P_s)^4+3(1-P_s)^{3+\mathrm{CR}}P_s\right)^{\left\lceil \frac{L_p}{4\mathrm{SF}} \right\rceil}]}{\mathrm{TP}\times(4+\mathrm{CR})2^{\mathrm{SF}}}, \mathrm{CR} = \frac{4}{7}, \frac{4}{8}. \end{cases} \tag{15}$$

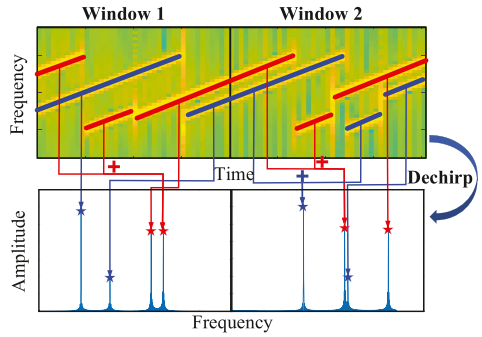

Fig. 2. The receiver uses an unaligned window to decompose collision packets by converting packet time offsets into frequency domain features.

1) Choose a Misaligned Window: In LoRa, the base upchirp $s(t)$ can be represented as $s(t) = e^{j2\pi(-\frac{BW}{2}+\frac{kt}{2})t}$, where T is the length of chirp and $k = \frac{BW}{T}$ is the slope. An encode chirp symbol is an upchirp with a frequency shift f, denoted as $x(t) = He^{j2\pi ft}s(t)$, where H is the signal amplitude. When a collision occurs, we select reception windows to divide the received signal into segments with length of T, but the reception window we choose is not aligned with the packet. Denoting τ as the time offset between the packet start and the reception window, the first chirp segment $x_1(t)$ can be written as

$$\begin{aligned} x_1(t) &= x(t-\tau) \\ &= He^{j2\pi(-f\tau+(f-k\tau)t)}s(t) \quad \tau \le t < T. \end{aligned} \tag{17}$$

Similarly, the second segment $x_2(t)$ can be written as

$$x_2(t) = He^{j2\pi(f(T-\tau)+(f+k(T-\tau))t)}s(t) \quad 0 < t < \tau \tag{18}$$

2) Extracting the Peak Point: For $x_1(t)$ in the first reception window, after multiplying with the downchirp $s^*(t)$, we have

$$\tilde{x}_1(t) = He^{j2\pi(-f\tau+(f-k\tau)t)} \quad \tau \le t < T. \tag{19}$$

Performing the fast Fourier transform (FFT) on $\tilde{x}_1(t)$ leads to

$$X_1[m] = \sum_{n=0}^{N_1-1} He^{j2\pi(-f\tau+(f-k\tau-m)\frac{n}{N})} \tag{20}$$

where $\tilde{x}_1[n]$ is nth sampling point of $\tilde{x}_1(t)$. N_1 and N represent the number of samples for the first chirp segment and the whole demodulation window, respectively. When the sampling rate is f_s, we have $N_1 = (T-\tau)f_s$ and $N = Tf_s$. Therefore, the amplitude is maximized at the frequency of $m = f - k\tau$ and the height of its peak is $h_1 = |X_1[m]| = H \times N_1 = Hf_s(T-\tau)$. Likewise, for $x_2(t)$ in the second window, we get

$$\tilde{x}_2(t) = He^{j2\pi(f(T-\tau)+(f+k(T-\tau))t)} \quad 0 < t < \tau, \tag{21}$$

$$X_2[m] = \sum_{n=0}^{N_2-1} He^{j2\pi(f(T-\tau)+(f+k(T-\tau)-m)\frac{n}{N})}, \tag{22}$$

where $\tilde{x}_2[n]$ is nth sampling point of $\tilde{x}_2(t)$. $N_2 = \tau f_s$ represents the number of samples for the second chirp segment. The amplitude is also maximized at $m = f - k\tau$ and the peak height is $h_2 = Hf_s\tau$. The above conclusions are well corroborated in Fig. 2. The computational complexity of FFT operation is $O(N\log(N))$. Since all Q windows need to perform FFT operations, the total computational complexity of this step is $O(QN\log(N))$.

3) Cluster the Peaks Into Multiple Groups: By matching peaks of the same frequency in two consecutive windows, we can pair these peaks. For each pair of peaks, we calculate the peak ratio $P = \frac{h_2}{h_1} = \frac{\tau}{T-\tau}$. It can be seen that P is determined by the window offset τ. Thus, P is identical for all chirps of the same packet, while it is distinct for chirps of different packets. There are Q consecutive windows, so the P-value needs to be solved QR times, i.e., the computational complexity is $O(QR)$. We use a k-means approach to group the peaks into R different clusters, each of which corresponds to a collided packet. The complexity of the k-means clustering algorithm can be expressed as $O(I(R+2QR\cdot R+QR))$. Together with the complexity of computing P, the total computational complexity of grouping the peaks is $O(I(R+2QR^2+2QR))$.

4) Resolve Peak Frequency Deviation: After obtaining the symbol peaks in each packet, we need to address the peak frequency deviation due to the window time offset. We use the base upchirps in the preamble to calculate the frequency shift and compensate for the frequency peaks of each demodulated symbol. Finally, we can decode the packet with a set of peaks using a standard LoRa decoder. Since it is necessary to compensate for the frequency bias of the QR peaks, the computational complexity is $O(QR)$.

In summary, the total computational complexity of collision decoding algorithm is $O(QN\log(N)+I(R+2QR^2+2QR)+QR)$, which is comparable to existing methods such as Choir [11], FTrack [12], OCT [13], and Magnifier [14]. For standard LoRa demodulation, the computational complexity mainly comes from the FFT operation which is $O(QN\log(N))$. Compared with it, the complexity of EnergySaver is higher by $O(I(R+2QR^2+2QR)+QR)$. However, since R, Q, and I are typically much smaller than N, the complexity does not increase significantly. In addition, all of the computational overhead introduced by collision decoding occurs at the gateway without any modifications to the LoRa end nodes.

IV. Numerical Results

A. Simulation Setup

The goal of EnergySaver is to achieve optimal EE for LoRa-based WUSNs by selecting the appropriate physical layer parameters. We perform a series of simulations to verify the effectiveness of our proposed mechanism. We set the soil parameters to $S = 51\%$ and $C = 9\%$. The gateway height h_a is set to 0.5m and the LoRa nodes operate at f_c = 915 MHz. The LoRa packets have a 10-byte payload with no cyclic redundancy check. To reduce information redundancy, we set CR to 4/5. The range of values for each parameter is $\mathrm{TP}_{\mathrm{list}} = \{2-20\}$dBm, $\mathrm{SF}_{\mathrm{list}} = \{7-12\}$, and $\mathrm{BW}_{\mathrm{list}} = \{125, 250, 500\}$kHz, which results in a total of $19 \times 6 \times 3 = 342$ combinations. The daily soil moisture dataset of Qinghai Lake Basin obtained from the National Tibetan Plateau Data Center is used as the VWC input [15]. To demonstrate the superiority of EnergySaver, we compare it with the existing schemes: standard ADR [7], ND-ADR [8], and ALPPS [5].

B. Simulation Results

The TP and SF settings obtained using EnergySaver, ALPPS, ADR, and ND-ADR algorithms are shown in Fig. 3. All algorithms use soil moisture data from the last day of each month, with the burial depth h_u set to 0.4 m and the horizontal distance set to 50 m. As expected, the TP and SF of the four algorithms increase in different magnitudes as the rainfall rises from winter to summer. However, they are very different in terms of parameter settings. The ALPPS algorithm tends to choose a larger TP and a smaller SF, even interrupting the transmission in July when soil moisture is high. The ADR and ND-ADR algorithms choose

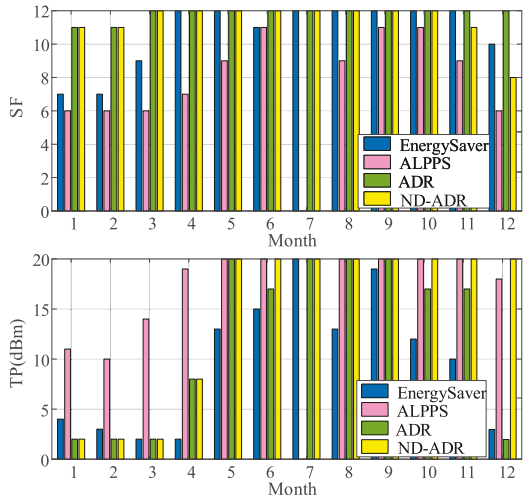

Fig. 3. TP and SF settings of EnergySaver, ALPPS, ADR, and ND-ADR under different VWC.

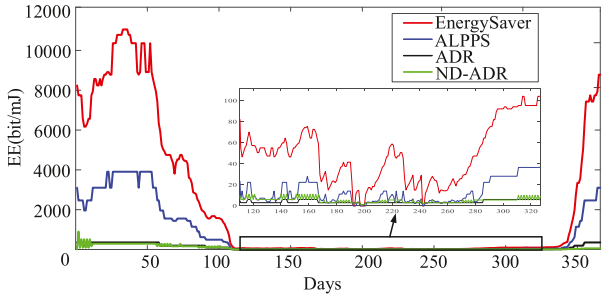

Fig. 4. EE of EnergySaver, ALPPS, ADR, and ND-ADR under different VWC.

similarly, with larger TP and SF. Especially during the months from July to September when rainfall is high, both algorithms consistently maintain the highest energy configurations of SF = 12 and TP = 20 dBm to ensure transmission reliability. Unlike these three approaches, the EnergySaver algorithm chooses more moderate values of TP and SF.

Furthermore, the EE performance of the four algorithms are compared. In Fig. 4, we observe that the attenuation is not severe during the winter months when the soil moisture is low, and thus the EE of both EnergySaver and ALPPS are relatively high. However, during months with high rainfall, such as May to September, both EE drop significantly, with ALPPS even experiencing frequent transmission outages. On the other hand, the parameter configurations of the ADR algorithm vary less with soil moisture and have consistently lower EE, whereas the parameter configurations of the ND-ADR algorithm change more frequently than ADR, but the overall trends are similar. In general, EnergySaver significantly outperforms ALPPS, ADR, and ND-ADR under all soil moisture conditions, with an average EE that is more than 20 times higher than that of ADR and ND-ADR, and nearly 2 times higher than that of ALPPS. EnergySaver slightly sacrifices PDR to improve EE, but the PDR stays above 90% most of the time. Among these four methods, EnergySaver not only significantly improves EE, but also guarantees the reliable communication simultaneously.

Since none of the three comparison schemes consider collisions, it is sufficient to compare the symbol error rate (SER) performance of EnergySaver with conventional LoRa demodulation. As shown in Fig. 5(a), EnergySaver has a low SER < 0.1 when packets collide

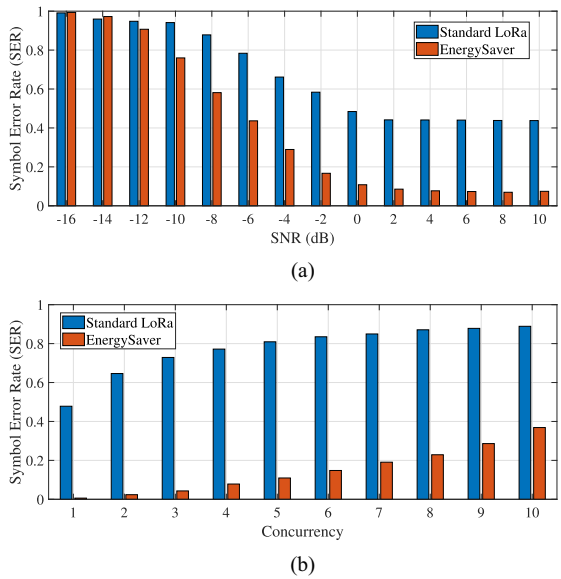

Fig. 5. The average SER performance in packet collisions. (a) The averaged SER of two packet collisions with different SNR. (b) The average SER performance as the concurrent nodes increase.

at relatively high SNR (> 10 dB). As the SNR decreases, the SER increases for both, but EnergySaver always outperforms conventional LoRa. We also verify the scalability of EnergySaver by decoding LoRa collisions with different numbers of concurrent transmissions. Fig. 5(b) shows the SER of standard LoRa and EnergySaver, both of which increase as the number of concurrent nodes increases from 1 to 10. However, the SER of EnergySaver increases much slower than that of standard LoRa, because the latter does not perform collision decoding and can only obtain information from the packet with highest SNR. For EnergySaver, we utilize windows to segment the chirps, focusing on peak frequency and height features, and therefore can distinguish packets more robustly. When the number of collision packets reaches 10, the SER of standard LoRa is up to 90%, which is 2.3× compared with that of EnergySaver (37%). EnergySaver can effectively reduce packet loss and retransmission during large concurrent data transmissions, ensuring that high EE is not compromised.

V. Conclusion

In this paper, we propose EnergySaver, an adaptive LoRa PHY parameter selection mechanism for LoRa-based WUSNs to achieve optimal EE. For each parameter configuration scheme, EnergySaver can obtain SNR based on underground channel model and the known soil properties. Using SNR and LoRa PHY parameters, PDR can be further characterized and the EE can be finally calculated. The optimal parameter configuration for the current channel state can be obtained by choosing the combination that maximizes EE. If multiple nodes send packets to the gateway concurrently, the low-complexity collision decoding algorithm is performed using unaligned windows. Simulation results show that our proposed EnergySaver mechanism is feasible compared to existing scheme, and can improve EE more than two times while guaranteeing transmission reliability. In addition, the EE performance is robust when EnergySaver is further extended to large-scale LoRa-WUSN scenarios. With high EE, low computational complexity, and strong collision decoding capability, EnergySaver has

significant advantages and strong scalability in a variety of application scenarios, such as agricultural soil information monitoring, geologic disaster prediction, and public facility monitoring.

REFERENCES

[1] H. Guo, "RSS-based localization for wireless underground battery-free sensor networks," *IEEE Sensors Lett.*, vol. 6, no. 10, Oct. 2022, Art. no. 7004104.

[2] G. Liu, "Data collection in MI-assisted wireless powered underground sensor networks: Directions, recent advances, and challenges," *IEEE Commun. Mag.*, vol. 59, no. 4, pp. 132–138, Apr. 2021.

[3] B. Zhou, V. S. S. L. Karanam, and M. C. Vuran, "Impacts of soil and antenna characteristics on LoRa in Internet of underground Things," in *Proc. IEEE Glob. Commun. Conf.*, Dec. 2021, pp. 1–6.

[4] G. Zhao, K. Lin, D. Chapman, N. Metje, and T. Hao, "Optimizing energy efficiency of LoRaWAN-based wireless underground sensor networks: A multi-agent reinforcement learning approach," *Internet Things J.*, vol. 22, Jul. 2023, Art. no. 100776.

[5] K. Lin and T. Hao, "Adaptive selection of transmission configuration for LoRa-based wireless underground sensor networks," in *Proc. IEEE Wireless Commun. Netw. Conf.*, Mar. 2021, pp. 1–6.

[6] H. Zhang, G. Liu, Y. Xu, and T. Jiang, "LoRaAid: Underground joint communication and localization system based on LoRa technology," *IEEE Trans. Wireless Commun.*, vol. 23, no. 5, pp. 5248–5260, May 2024.

[7] Semtech Corporation, *LoRaWAN—Simple Rate Adaptation Recommended Algorithm*," Camarillo, CA, USA: Semtech, 2016.

[8] C. Jiang, Y. Yang, X. Chen, J. Liao, W. Song, and X. Zhang, "A new-dynamic adaptive data rate algorithm of LoRaWAN in harsh environment," *IEEE Internet Things J.*, vol. 9, no. 11, pp. 8989–9001, Jun. 2022.

[9] Z. Sun, I. F. Akyildiz, and G. P. Hancke, "Dynamic connectivity in wireless underground sensor networks," *IEEE Trans. Wireless Commun.*, vol. 10, no. 12, pp. 4334–4344, Dec. 2011.

[10] Y. Li, J. Yang, and J. Wang, "DyLoRa: Towards energy efficient dynamic LoRa transmission control," in *Proc. IEEE Conf. Comput. Commun.*, Jul. 2020, pp. 2312–2320.

[11] R. Eletreby, D. Zhang, S. Kumar, and O. Yağan, "Empowering low-power wide area networks in urban settings," in *Proc. Conf. ACM Special Int. Group Data Commun.*, 2017, pp. 309–321.

[12] X. Xia, Y. Zheng, and T. Gu, "FTrack: Parallel decoding for LoRa transmissions," *IEEE/ACM Trans. Netw.*, vol. 28, no. 6, pp. 2573–2586, Dec. 2020.

[13] Z. Wang, L. Kong, K. Xu, L. He, K. Wu, and G. Chen, "Online concurrent transmissions at LoRa gateway," in *Proc. IEEE Conf. Comput. Commun.*, 2020, pp. 2331–2340.

[14] W. Chen, S. Wang, and T. He, "Magnifier: Leveraging the fine-grained hardware information and their temporal patterns for concurrent LoRa decoding," *IEEE. Trans. Mob. Comput.*, vol. 23, no. 5, pp. 4362–4375, May 2024.

[15] X. Li, "Daily soil temperature and moisture dataset in a small catchment of Qinghai Lake Basin (2019–2021)," Nat. Tibetan Plateau / Third Pole Environ Data Center, 2022. [Online]. Available: https://www.tpdc.ac.cn/en/data/9ade5938-0e47-4697-a807-52dfd33c210f/